Electronic Supplementary Information

Metal-organic-framework-engaged formation of Co nanoparticles-embedded carbon@Co_9S_8 double-shelled nanocages for efficient oxygen reduction

Han Hu,[a] Lei Han,[a] Mengzhou Yu,[b] Zhiyu Wang[b] and Xiong Wen (David) Lou*[a]*

[a] *School of Chemical and Biomedical Engineering, Nanyang Technological University, 62 Nanyang Drive, Singapore, 637459, (Singapore)* E-mail: xwlou@ntu.edu.sg; davidlou88@gmail.com;

Webpage: http://www.ntu.edu.sg/home/xwlou/

[b]*Carbon Research Laboratory, School of Chemical Engineering, State Key Lab of Fine Chemicals, Dalian University of Technology, Dalian, Liaoning, 116024, China* Email: zywang@dlut.edu.cn

Experimental details

Synthesis of ZIF-67 polyhedrons: In a typical synthesis, two solutions were prepared by dissolving $Co(NO_3)_2$ $6H_2O$ (291 mg) and 2-methylimidazole (328 mg) in 25 mL of methanol, respectively. Then, the two solutions were mixed rapidly and aged for 24 h at room temperature. The precipitate was washed by ethanol for 4 times before vacuum dried at room temperature overnight.

Synthesis of ZIF-67@a-CoS yolk-shell structures: 40 mg of ZIF-67 particles was dispersed in 40 mL of ethanol under ultrasonic, followed by adding 0.18 g of thioacetamide (TAA) and refluxing at 90 ^oC for 12 min. Afterwards, the products were harvested by several rinsing-centrifugation cycles. By prolonging the reaction time to 30 min, *a*-CoS nanocages with entirely hollow cavity can be obtained.

Synthesis of Co-C@Co_9S_8 DSNCs: The Co-C@Co_9S_8 DSNCs were fabricated by annealing ZIF-67@a-CoS yolk-shell structures in nitrogen flow for 2 h at 600 ^oC with a ramp rate of 1 ^oC

min^{-1}. For comparison, Co-C polyhedrons and Co_9S_8 nanocages were also prepared by annealing ZIF-67 particles and *a*-CoS nanocages under similar conditions, respectively.

Materials Characterization: X-ray diffraction (XRD) patterns were collected on a Bruker D2 Phaser X-Ray Diffractometer with Ni filtered Cu *Kα* radiation (λ = 1.5406 Å) at a voltage of 30 kV and a current of 10 mA. Field-emission scanning electron microscopy (FESEM; JEOL, JEM-6700F, 5 kV) and transmission electron microscopy (TEM; JEOL, JEM-1400/JEM-2010, 200 kV) were utilized to analyze the microstructures of different samples. The nitrogen adsorption-desorption isotherms of Co-C@Co_9S_8 DSNCs, Co-C polyhedrons and Co_9S_8 nanocages were recorded with a Quantachrome Autosorb AS-6B system.

Electrochemical Measurements: The electrocatalytic activity of the samples was examined by using a three-electrode system with a PARSTAT MC potentiostat/galvanostat workstation. A polished glass carbon (GC) disk electrode was used as a support. The catalyst suspension was prepared by dispersing 5 mg of the catalyst in 1 mL of ethanol under sonication. In order to prepare the working electrode, 15 μL of the suspension was pipetted on the surface of GC electrode, followed by dropping another 5 μL of Nafion solution (0.5 wt.%) to glue the catalyst on the surface of GC electrode. The counter electrode and reference electrode were a Pt wire and a saturated calomel electrode (SCE), respectively. All the measured potentials were referred to reversible hydrogen electrode (RHE) with following equation:

$$E(\text{RHE}) = E(\text{SCE}) + (0.242+0.059\ \text{pH})\text{V}$$

The cyclic voltammetry (CV) measurements for Co-C polyhedrons, Co-C@Co_9S_8 DSNCs and 20 wt.% Pt/C in both Ar- and O_2-saturated KOH solutions were performed in the potential range of 0 to 1.2 V with a scan rate of 10 mV s^{-1} while other CV curves were recorded in the potential range

of 0 to 1 V. Furthermore, the CV curves of the Co-C@Co_9S_8 DSNCs at scan rates of 20, 50 and 100 mV s^{-1} in O_2-saturated KOH solutions were also recorded. For comparison of the effect of methanol crossover, the CV curves of Co-C@Co_9S_8 DSNCs and 20 wt.% Pt/C in O_2-saturated mixture solution containing KOH and methanol (KOH, 0.1 M; methanol, 3.0 M) were conducted. The polarization curves for ORR were conducted at various rotation speeds from 400 to 2,500 rpm with a scan rate of 10 mV s^{-1}. The *I-t* curves were tested in O_2-saturated solution under a fixed potential with a rotation speed of 1600 rpm. Before testing, the electrodes were cycled at 100 mV s^{-1} until reproducible CV curves were obtained.

On the basis of the RDE data, the electron transfer number (n) was calculated from the Koutecky–Levich (K-L) equation:

$$1/j = 1/j_k + 1/B\omega^{1/2}$$

Where j_k is the kinetic current and ω represents the rotation speed. *B* can be determined from the slope of the K-L plots. Then, n can be obtained via the followed equation:

$$n=\mathrm{B}/(0.2F(Do_2)^{2/3}(\upsilon)^{-1/6}Co_2)$$

where *F* is Faraday constant (96485 C mol^{-1}), Do_2 is the diffusion coefficient of O_2 (1.9×10^{-5} cm^2 s^{-1}), υ is the kinetic viscosity (υ = 0.01 cm^2 s^{-1}) and Co_2 is the bulk concentration of O_2 (1.2×10^{-6} mol cm^{-3}). When expressing the rotation speed in rpm, the constant 0.2 is applied.

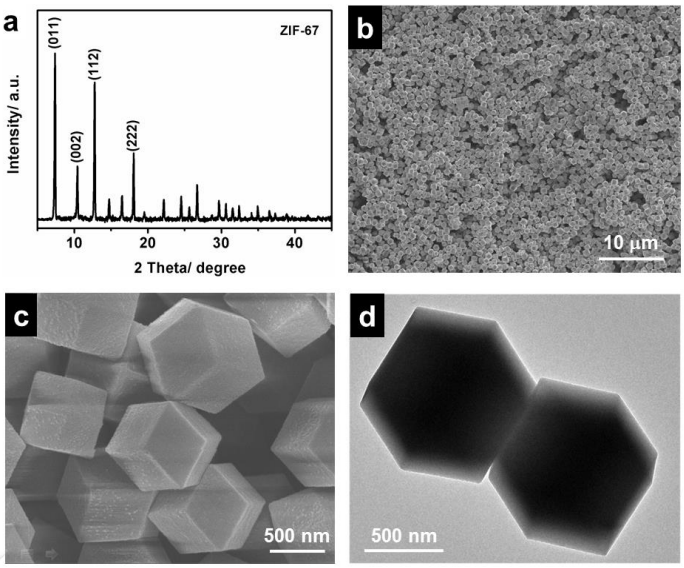

Fig. S1 (a) XRD pattern of ZIF-67 polyhedrons; (b, c) FESEM images of ZIF-67 polyhedrons; (d) TEM image of ZIF-67 polyhedrons.

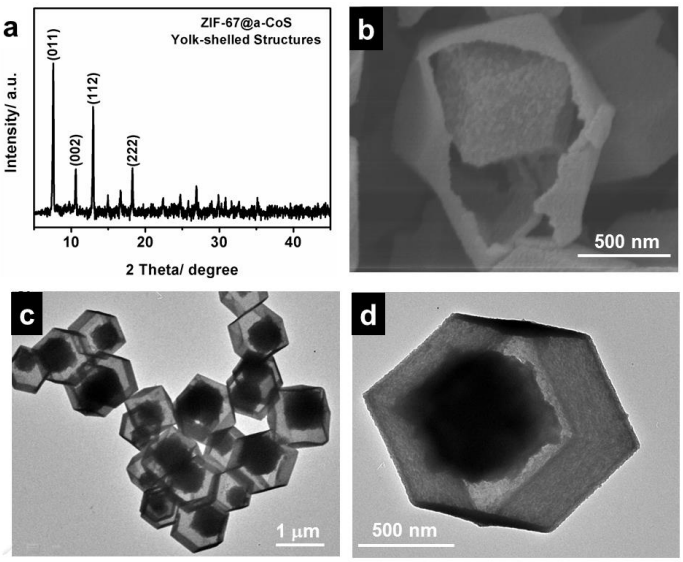

Fig. S2 (a) XRD pattern of ZIF-67@a-CoS yolk-shell structures; (b) FESEM image of an individual yolk-shell structure with broken shell; (c, d) TEM images of ZIF-67@a-CoS yolk-shell structures.

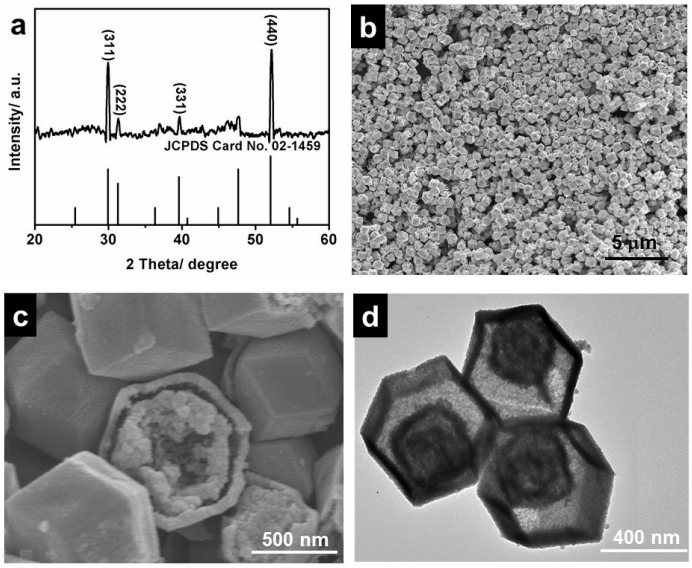

Fig. S3 (a) XRD pattern of Co-C@Co_9S_8 DSNCs; (b) FESEM images of Co-C@Co_9S_8 DSNCs; (c) FESEM image of an individual Co-C@Co_9S_8 nanocage with broken shell; (d) TEM image of Co-C@Co_9S_8 DSNCs.

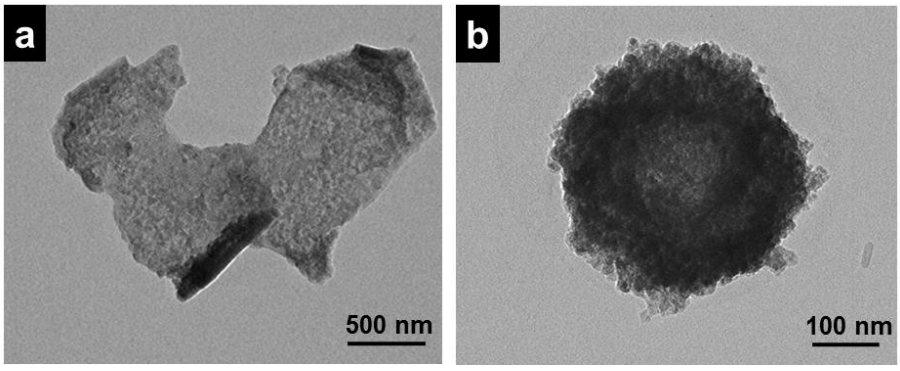

Fig. S4 TEM images of (a) outer Co_9S_8 shell and (b) inner Co-C nanocage. They were obtained by breaking the Co-C@Co_9S_8 DSNCs under strong ultrasonic.

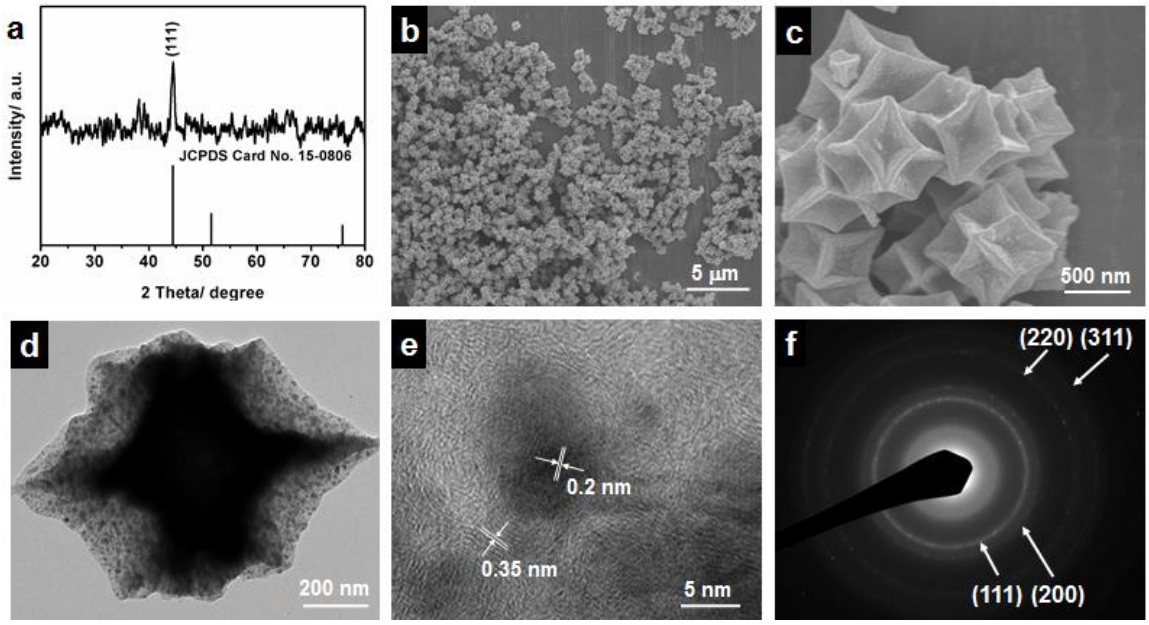

Fig. S5 (a) XRD pattern, (b, c) FESEM images, (d) TEM image, (e) HRTEM image, and (f) SAED pattern of concave Co-C polyhedrons, which were obtained by directly annealing ZIF-67 polyhedrons at 600 ^{o}C in nitrogen flow.

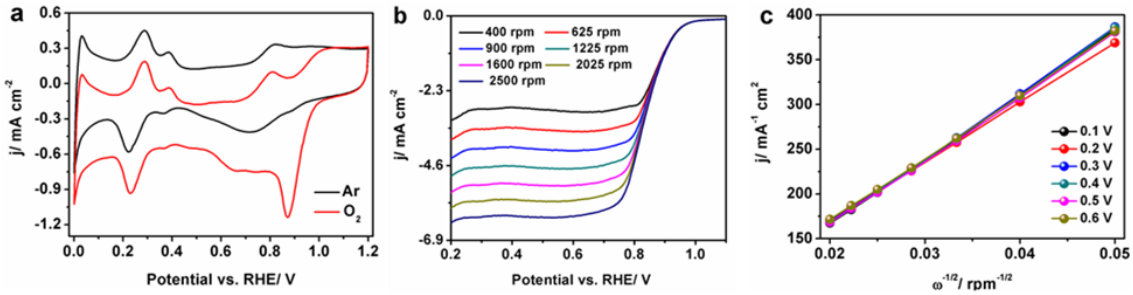

Fig. S6 (a) CV curves of a commercial 20 wt.% Pt/C catalyst in Ar- and O_2-saturated 0.1 M KOH solution; (b) LSV curves of Pt/C catalyst at different rotation rates; (c) Koutecky–Levich plots of Pt/C catalyst at various potentials.

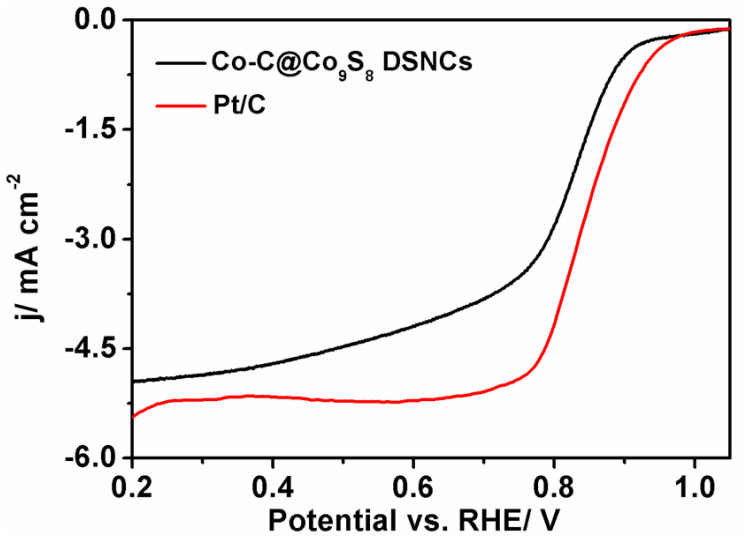

Fig. S7 Comparison of the LSV curves of Co-C@Co_9S_8 DSNCs and Pt/C at the rotation speed of 1600 rpm.

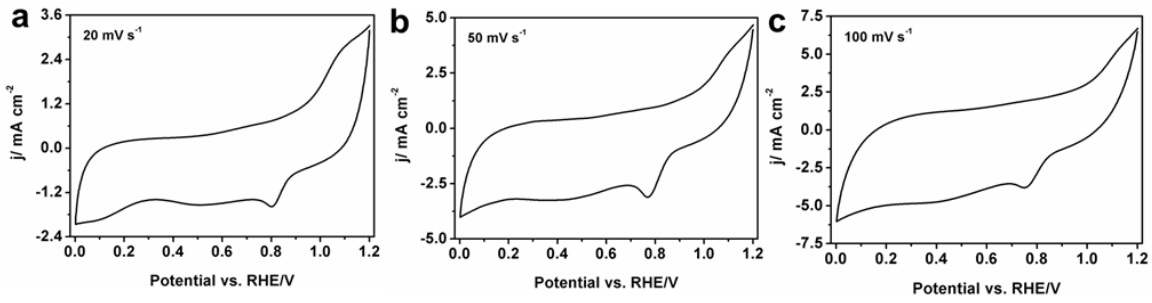

Fig. S8 CV curves of Co-C@Co_9S_8 DSNCs in O_2-saturated 0.1 M KOH solution at scan rates of (a) 20, (b) 50 and (c) 100 mV s^{-1}.

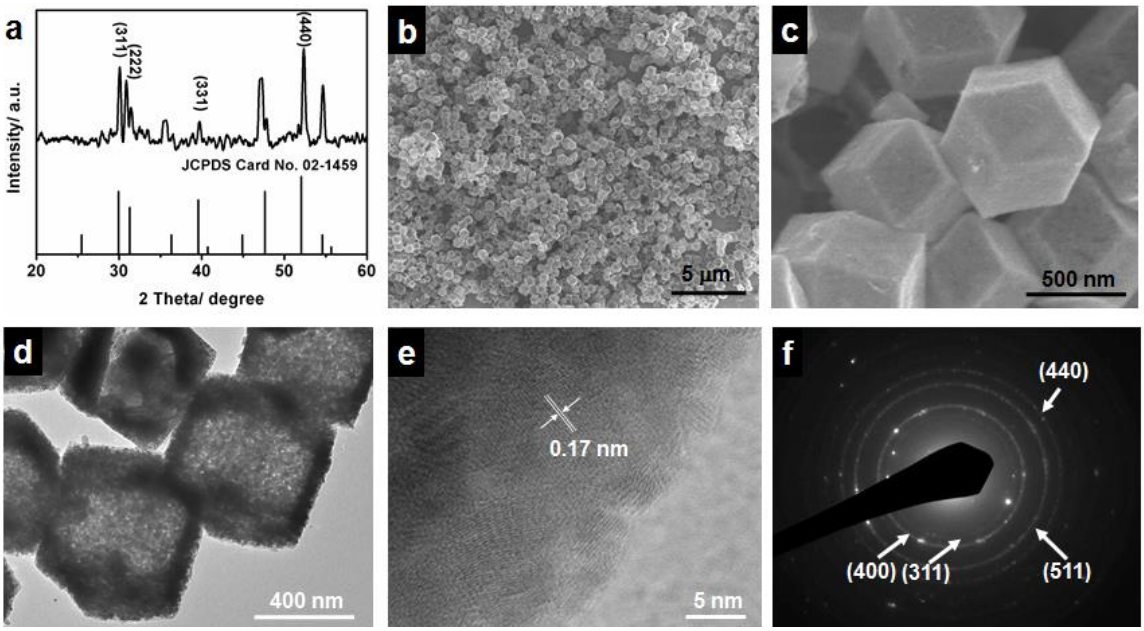

Fig. S9 (a) XRD pattern, (b, c) FESEM images, (d) TEM image, (e) HRTEM image, and (f) SAED pattern of Co_9S_8 nanocages, which were obtained by directly annealing a-CoS nanocages at 600 ^oC in nitrogen flow.

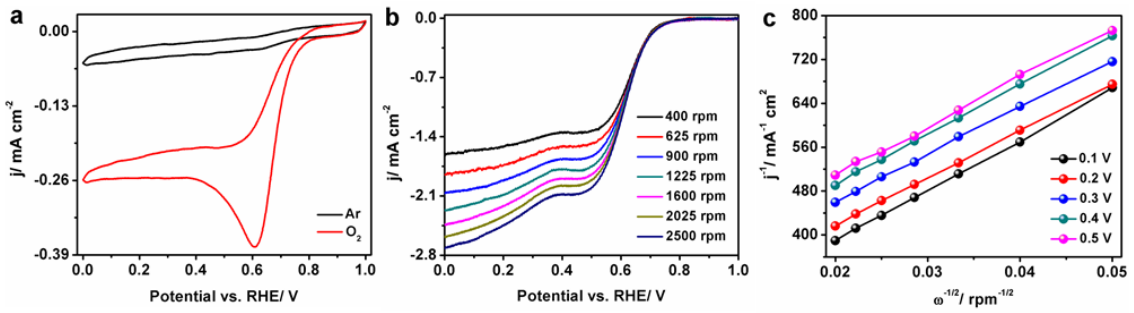

Fig. S10 (a) CV curves of Co_9S_8 nanocages in Ar- and O_2-saturated 0.1 M KOH solution; (b) LSV curves of Co_9S_8 nanocages at different rotation rates; (c) Koutecky–Levich plots of Co_9S_8 nanocages at various potentials.

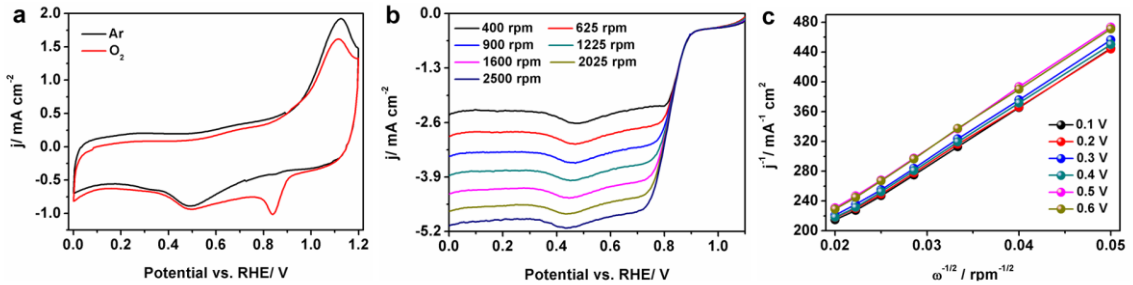

Fig. S11 (a) CV curves of Co-C polyhedrons in Ar- and O_2-saturated 0.1 M KOH solution; (b) LSV curves of Co-C polyhedrons at different rotation rates; (c) Koutecky–Levich plots of Co-C polyhedrons at various potentials.

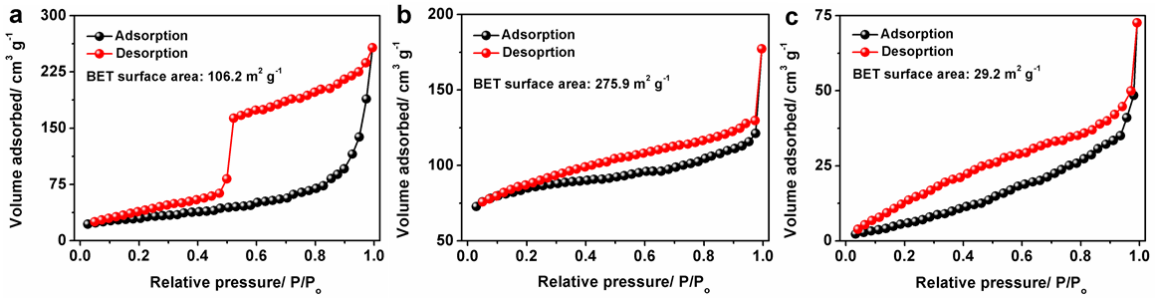

Fig. S12 Nitrogen adsorption-desorption isotherms of Co-C@Co_9S_8 DSNCs (a), Co-C polyhedrons (b), and Co_9S_8 nanocages (c) at 77 K.

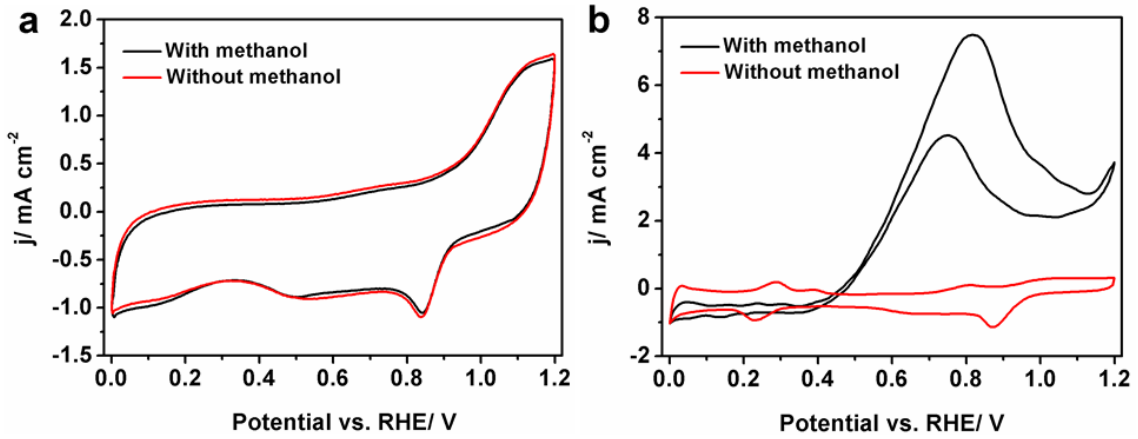

Fig. S13 CV curves of (a) Co-C@Co_9S_8 DSNCs and (b) Pt/C in O_2-saturated KOH solution (0.1 M) and O_2-saturated mixture solution (KOH, 0.1 M; Methanol, 3 M).

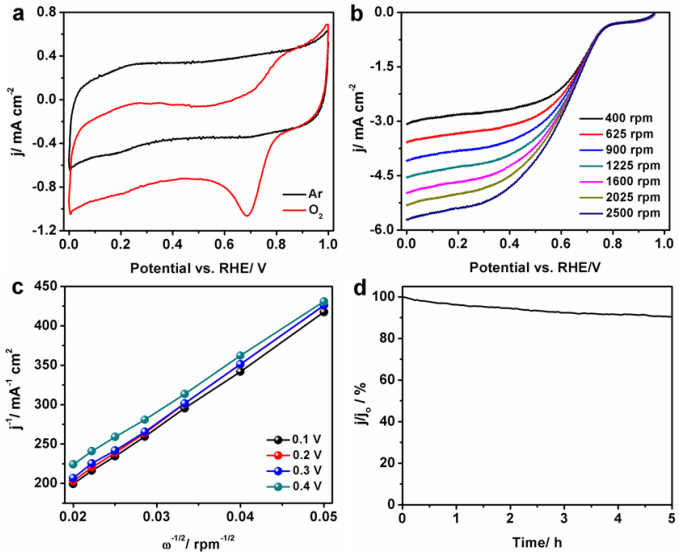

Fig. S14 (a) CV curves of Co-C@Co_9S_8 DSNCs in Ar- and O_2-saturated 0.1 M $HClO_4$ solution at a scan rate of 10 mV s^{-1}; (b) LSV curves of Co-C@Co_9S_8 DSNCs at different rotation rates; (c) Koutecky–Levich plots of Co-C polyhedrons at various potentials; (d) Chronoamperometric responses of Co-C@Co_9S_8 DSNCs at 0.4 V in O_2-saturated 0.1 M $HClO_4$ solution at 1600 rpm.

Table S1 Comparison of the electrocatalytic activity of Co-C@Co_9S_8 DSNCs with some newly reported electrocatalysts

Catalyst	Onset Potential/V	Cathodic peak potential/V	Electrolyte	Scan rate/ mV s^{-1}	Reference
Fe_3O_4/N-GAs	0.774	0.624	0.1 M KOH	100	1
g-C_3N_4@CMK-3	--	0.714	0.1 M KOH	--	2
N-S-G	--	0.724	0.1 M KOH	100	3
N-CG-CoO	--	0.753	1 M KOH	50	4
N-carbon nanosheets	--	0.73	0.1 M KOH	50	5
N-carbon nanocages	0.834	0.744	0.1 M KOH	10	6
N-carbon	--	0.776	0.1 M KOH	10	7
$NiCo_2S_4$@N/S-rGO	0.854	0.744	0.1 M KOH	20	8
G-CN800	--	0.714	0.1 M KOH	100	9
Co-C@Co_9S_8 DSNCs	0.96	0.83	0.1 M KOH	10	This work
Co-C@Co_9S_8 DSNCs	0.91	0.80	0.1 M KOH	20	This work
Co-C@Co_9S_8 DSNCs	0.89	0.77	0.1 M KOH	50	This work
Co-C@Co_9S_8 DSNCs	0.87	0.75	0.1 M KOH	100	This work
Pt/C	1.05	0.87	0.1 M KOH	10	This work

Table S2 Comparison of current densities of samples at different potentials and rotation speeds

Sample	Current density / mA cm^{-2}				Reference
	0.4 V		0.5 V		
	2500 rpm	1600 rpm	2500 rpm	1600 rpm	
Co-C@Co_9S_8 DSNCs	5.3	4.71	5.05	4.50	This work
G-Co/CoO	5.1	4.4	4.95	4.32	10
Carbon-L	--	3.72	--	3.51	5
Co_3S_4/G	--	3.17	--	2.99	11

Supplementary References

1. Z. S. Wu, S. Yang, Y Sun, K. Parvez, X. L. Feng, K. Müllen, *J. Am. Chem. Soc.*, 2012, **134**, 9082.
2. Y. Zheng, Y. Jiao, J. Chen, J. Liu, J. Liang, A. Du, W. M. Zhang, Z. H. Zhu, S. C. Smith, M. Jaroniec, G. Q. Lu, S. Z. Qiao, *J. Am. Chem. Soc.,* 2011, **133**, 20116.
3. J. Liang, Y. Jiao, M. Jaroniec, S. Z. Qiao, *Angew. Chem. Int. Ed.,* 2012, **51**, 11496.
4. S. Mao, Z. Wen, T. Huang, Y. Hou, J. H. Chen, *Energy Environ. Sci.*, 2014, **7**, 609.
5. P. Zhang, F. Sun, Z. H. Xiang, Z. G. Shen, J. Yun, D. P. Cao, *Energy Environ. Sci.*, 2014, **7**, 442.
6. S. Chen, J. Bi, Y. Zhao, L. Yang, C. Zhang, Y. Ma, Q. Wu, X. Wang, Z. Hu, *Adv. Mater.*, 2012, **24**, 5593.
7. S. Gao, K. Geng, H. Liu, X. Wei, M. Zhang, P. Wang, J. Wang, *Energy Environ. Sci.*, 2015, **8**, 221.
8. Q. Liu, J. Jin, J. Zhang, *ACS Appl. Mater. Interfaces*, 2013, **5**, 5002.
9. S. Yang, X. L. Feng, X. Wang, K. Müllen, *Angew. Chem. Int. Ed.*, 2011, **50**, 5339.
10. S. J. Guo, S. Zhang, L. H. Wu, S. H. Sun, *Angew. Chem. Int. Ed.*, 2012, **51**, 11770.
11. N. Mahmood, C. Z. Zhang, J. Jiang, F. Liu, Y. L. Hou, *Chem. Eur. J.*, 2013, **19**, 5183.